Biogeosciences

Impact of seawater [Ca^{2+}] on the calcification and calcite Mg / Ca of *Amphistegina lessonii*

A. Mewes[1], G. Langer[2], S. Thoms[1], G. Nehrke[1], G.-J. Reichart[3,4], L. J. de Nooijer[3], and J. Bijma[1]

[1]Alfred Wegener Institute, Helmholtz Centre for Polar and Marine Research, Am Handelshafen 12, 27570 Bremerhaven, Germany
[2]Department of Earth Sciences, Cambridge University, Downing St., Cambridge, CB2 3EQ, UK
[3]Royal Netherlands Institute for Sea Research, Landsdiep 4, 1797 SZ 't Horntje, Texel, the Netherlands
[4]Department of Earth Sciences, Utrecht University, Budapestlaan 4, 3584 CD Utrecht, the Netherlands

Correspondence to: A. Mewes (antje.mewes@awi.de)

Abstract. Mg / Ca ratios in foraminiferal tests are routinely used as paleotemperature proxies, but on long timescales, they also hold the potential to reconstruct past seawater Mg / Ca. The impact of both temperature and seawater Mg / Ca on Mg incorporation in Foraminifera has been quantified by a number of studies. The underlying mechanism responsible for Mg incorporation in foraminiferal calcite and its sensitivity to environmental conditions, however, has not been fully identified. A recently published biomineralization model (Nehrke et al., 2013) proposes a combination of transmembrane transport and seawater leakage or vacuolization to link calcite Mg / Ca to seawater Mg / Ca and explains interspecies variability in Mg / Ca ratios. To test the assumptions of this model, we conducted a culture study in which seawater Mg / Ca was manipulated by varying [Ca^{2+}] and keeping [Mg^{2+}] constant. Foraminiferal growth rates, test thickness and calcite Mg / Ca of newly formed chambers were analyzed. Results showed optimum growth rates and test thickness at Mg / Ca closest to that of ambient seawater. Calcite Mg / Ca is positively correlated to seawater Mg / Ca, indicating that it is not absolute seawater [Ca^{2+}] and [Mg^{2+}] but their ratio that controls Mg / Ca in tests. These results demonstrate that the calcification process cannot be based only on seawater vacuolization, supporting the mixing model proposed by Nehrke et al. (2013). Here, however, we suggest transmembrane transport fractionation that is not as strong as suggested by Nehrke et al. (2013).

1 Introduction

Foraminiferal test Mg / Ca$_{CC}$ is a proxy used in paleoceanography to reconstruct past seawater temperatures (e.g., Nürnberg et al., 1996; Lear et al., 2000). In addition to temperature, calcite Mg / Ca$_{CC}$ is also controlled by seawater Mg / Ca$_{SW}$ (Segev and Erez, 2006; Evans and Müller, 2012). Since Mg / Ca$_{SW}$ varied over geological time due to changes in the balance between Mg and Ca input and output, paleoceanographers need to account for this ratio in seawater when using foraminiferal Mg / Ca$_{CC}$ to reconstruct temperatures on timescales beyond ~ 1 Myr. Due to the long residence times of Mg^{2+} (~ 13 Myr) and Ca^{2+} (~ 1 Myr), this ratio does not need to be corrected for when using foraminiferal Mg / Ca on shorter timescales (Broecker and Yu, 2011; Hardie, 1996).

Biological processes involved in calcification complicate the relationships between Mg / Ca$_{CC}$, temperature and Mg / Ca$_{SW}$, which is apparent from large inter-species differences in Mg / Ca (Bentov and Erez, 2006). To improve the reliability of proxy relationships, it is hence necessary to understand the impact of cellular processes involved in calcification. Controlled culture studies allow the disentanglement of variables that often covary in the field, as well as allowing seawater conditions to be more extreme than naturally occurring conditions. Studies by, e.g., Erez (2003), and Bentov et al. (2009) suggested that foraminifers vacuolize seawater to acquire the ions needed for calcification. Seawater vacuolization would require the extraction of Ca^{2+} and CO_3^{2-}

from the vacuoles or the removal of all unwanted ions, such as, e.g., Mg^{2+}. However, studies by De Nooijer et al. (2009) and Nehrke et al. (2013) showed that the volume of vacuoles observed during calcification cannot account for the total amount of ions needed for calcification. An intracellular storage reservoir for inorganic carbon, or a "pool", was shown to exist for the perforate foraminifer, *Amphistegina lobifera* (Ter Kuile et al., 1989), possibly corresponding to the vacuoles described by Erez (2003) (De Nooijer et al., 2014). However, Ca^{2+} pools are absent in the benthic *Ammonia aomoriensis*, as demonstrated by Nehrke et al. (2013). On the basis of their experiments, these authors suggested that selective transmembrane transport (TMT) is responsible for the delivery of Ca^{2+} to the site of calcification during chamber formation. A minor portion of unfractionated elements may reach the site of calcification passively via seawater leakage or via seawater vacuolization, a process summarized as passive transport (PT) (Nehrke et al., 2013). This model predicts a linear relationship between Mg / Ca$_{SW}$ and Mg / Ca$_{CC}$, as observed for, e.g., *Amphistegina lessonii* (Segev and Erez, 2006; Mewes et al., 2014), *Amphistegina lobifera* (Segev and Erez, 2006) and *Ammonia aomoriensis* (Mewes et al., 2014). In the experiments by Mewes et al. (2014), [Ca] was kept constant while [Mg] was varied. Verifying the TMT–PT model requires investigating the effect of varying seawater [Ca] on Mg / Ca$_{CC}$.

The aim of this culture study is to investigate the effect of different Mg / Ca$_{SW}$ on test growth, test wall thickness and Mg / Ca$_{CC}$ by varying seawater [Ca] and keeping [Mg] constant. The results allow testing the assumptions of the calcification model by Nehrke et al. (2013) and are used to construct a refined model.

2 Materials and methods

2.1 Sampling and storage of specimens

The benthic foraminifer *Amphistegina lessonii* was chosen for this experiment because our experience has shown that *A. lessonii* grow and reproduce well in our laboratory. Due to its relatively large size of > 1 mm, it is furthermore relatively easy to observe and handle. Because it was cost efficient and easily accessible, reef rubble with attached benthic Foraminifera was sampled in April 2012 from a coral reef aquarium at Burger's Zoo, Arnhem, the Netherlands (Ernst et al., 2011). Sampling foraminifers from the zoo aquarium instead of the natural environment does not seem ideal on the face of it. The zoo's aquarium is, however, one of the largest aquaria in the world, harboring a very rich (micro)fauna and providing spatially diverse microhabitats. In the present study we furthermore deal with a fairly fundamental aspect of physiology, namely with the response to concentrations and ratios of major ions in seawater. Zoo specimens had no opportunity to adjust their physiological machinery

to changing Mg and Ca, since these concentrations are the same in the aquarium as in the field. Upon return to the laboratory, samples were kept in an aquarium (AQUAEL 10), containing a heating element, a light source (light intensity $\sim 80 \, \mu mol \, m^{-2} \, s^{-2}$) and a small water pump with a filter to circulate the water. For the experiments, specimens of *Amphistegina lessonii* were collected from the rubble using a small brush (Sect. 2.3).

2.2 Preparation of culture media

From our experience with previous culture experiments we knew that some species of Foraminifera do not grow well in 100 % artificial seawater (ASW). A small pilot experiment, in which we cultured *Amphistegina lessonii* in different mixtures of artificial (ASW) and natural seawater (NSW), revealed that a mixture of 30 % NSW and 70 % ASW results in optimal foraminiferal growth rates. To prepare culture media with constant [Mg] but varying [Ca], elemental concentrations of the available NSW were determined. Based on this, the concentrations to be added to the ASW (based on the recipe by Kester et al., 1967) were calculated. Six different treatments with constant [Mg] (50 mM) and varying [Ca] (3, 5, 7, 10, 21, 38 mM) were prepared, resulting in media with Mg / Ca ratios of $\sim$ 16.6, 10, 7.1, 5, 2.4 and 1.5. Actual concentrations in the final culture media were verified by inductively coupled plasma–optical emission spectrometry (ICP-OES) and are summarized in Table 1. Since salinity varied, depending on the varying [Ca], salinity was measured for all treatments (salinometer: WTW, Cond 330) and adjusted to a constant value ($S = 32.4$) by adding NaCl from a stock solution (5 M). pH was measured using a pH meter (WTW, pH 3110, NBS scale) and adjusted to a constant value (pH = 8.01) by adding 1M NaOH. Total alkalinity (TA) and dissolved inorganic carbon (DIC) were determined using an SI Analytics TW alpha plus and an XY-2 Sampler (Bran und Luebbe), respectively. All values are summarized in Table 1.

2.3 Juvenile *Amphistegina lessonii*

For the culture experiment we used offspring, grown in culture, of the zoo-derived specimens. Offspring were used to ensure that most of their calcite is formed during incubation in controlled conditions. To obtain juveniles, adult specimens were picked from the stock material. Adult specimens crawled up the aquarium glass walls, facilitating the selection of living specimens, and were transferred to well plates. Well plates were placed in light- (12 h light–12 h dark cycle) and temperature-controlled incubators (RUMED, Rubarth Apparate GmbH) at 25 °C. The daylight sources had a light intensity of 130 $\mu mol \, m^{-2} \, s^{-1}$ at the level of the well plates. After a few days, about 10 % of the specimens had reproduced asexually. These juveniles were selected for the culturing experiments and evenly distributed between the different treatments.

Table 1. Details of culture media as well as morphological and chemical test parameters.

	Amphistegina lessonii					
	Treat. 1	Treat. 2	Treat. 3	Treat. 4	Treat. 5	Treat. 6
SW Mg^{2+} (mM)	51.64	52.56	52.75	52.66	52.05	52.40
SW Ca^{2+} (mM)	34.19	17.86	9.22	6.63	4.77	3.18
Mg / Ca$_{SW}$ (mol mol^{-1})±SE	1.51±0.00	2.94±0.03	5.72±0.02	7.95±0.05	10.91±0.07	16.47±0.09
Mg / Ca$_{CC}$ (mmol mol^{-1})±SE	22.95±0.81	40.79±1.38	52.08±1.72	67.50±2.37	83.35±1.96	–
T (°C)	25	25	25	25	25	25
S ‰	32.4	32.4	32.4	32.4	32.4	32.4
pH (NBS)	8.1	8.1	8.1	8.1	8.1	8.1
TA (µmol kg^{-1})	2615	2545	2504	2504	2492	2479
Ω (calcite)	16.75	8.74	4.49	3.24	2.33	1.55
DIC (µmol kg^{-1})	2302	2298	2286	2295	2294	2290
Final test size (µm) ±SE	362.7±9.3	503.4±9.1	427.5±6.4	341.1±5.9	240.6±7.9	138.4±7.8
Growth rate (µm day^{-1})±SE	4.21±0.36	8.15±0.46	6.91±0.84	5.89±0.13	2.95±0.91	−0.53±0.21
Mean SNW·1000 (µg µm^{-1})±SD	124.64±26.13	190.90±29.40	206.22±23.61	163.34±26.51	78.94±40.56	24.60±16.43

2.4 Culture experiment

The culture protocol was the same as reported in Mewes et al. (2014), except for the manipulation of the culture media (compare Sect. 2.2). Juveniles of *A. lessonii* were incubated in petri dishes, containing ~ 10 mL of culturing medium. In total, juveniles of four different broods were used and divided equally over the treatments (each brood in duplicates containing 5–10 individuals per petri dish), resulting in 50 to 56 juveniles for every treatment. To maintain constant culture conditions, the culture media was replaced once every 3 days. Immediately after the replacement of the media, specimens were fed 100 µL of a dense culture of the green algae *Dunaliella salina* ($\sim 4 \times 10^6$ cells mL^{-1}). To prevent bacterial colonization of petri dishes due to left-over food, all specimens were transferred to a clean petri dish once a week. This resulted in an occasional loss of some specimens. Dead specimens were identified by a change in color from brownish or greenish to pale or white, due to their loss of symbionts. Survival rates were high (ca. 95 %) and not correlated with any measured parameter. Dead specimens were removed from culture. The culture experiment ran for ~ 7 weeks and resulted in a final number of successfully grown juveniles of between 37 and 56 per treatment.

Alkalinity was determined once a week, and culture media element concentrations were measured a second time at the end of the experiment. Prior to analyses media were filtered (syringe filter 0.2 µm).

2.5 Determination of size and growth rates

The maximum test size (µm) of all specimens was measured weekly using a digital camera (AxioCam MRc5) connected to a Zeiss microscope (Axiovert 200M). Maximum test diameters were determined from pictures using the Axiovision (Zeiss) software. Foraminiferal test size increased with time and from the resulting regression, growth rates in microm-

eters per day were calculated. In Foraminifera, biomass increases continuously, whereas chamber formation is intermittent (e.g., Signes et al., 1993). Because we did not observe the duration of actual chamber formation, reported rates refer to overall growth rates, which should not be confused with calcium carbonate precipitation rates.

2.6 Cleaning procedure

After the termination of the experiment, all specimens were rinsed with distilled water and placed in a 7 % NaOCl solution for 4 h to remove organic material. Specimens were rinsed again and dried overnight (12 h) in an oven at 60 °C.

2.7 Determination of weight and size-normalized weight

Test weight was determined with an ultra microbalance (Mettler Toledo UMX2; precision: ±0.1 µg). Due to the limited weight of individual specimens, each replicate group was weighed as a whole, resulting in $n = 8$ (duplicates × four broods) measurements. The mean weight per specimen was determined by dividing the weight of each replicate by the number of specimens in the group. Weight was normalized to the final size measured with the microscope. This size-normalized weight (SNW) is an indication of test wall thickness and is defined by

$$\text{SNW} = \frac{\text{weight (µg)}}{\text{size (µm)}}. \tag{1}$$

Size-normalized weight also depends on the time spent in culture, which makes it challenging to compare SNW measured in our experiment to other experiments. Thus, we expressed size-normalized weight as relative SNW (%), such that it is related to the highest SNW in each of the experiments (which equals 100 %).
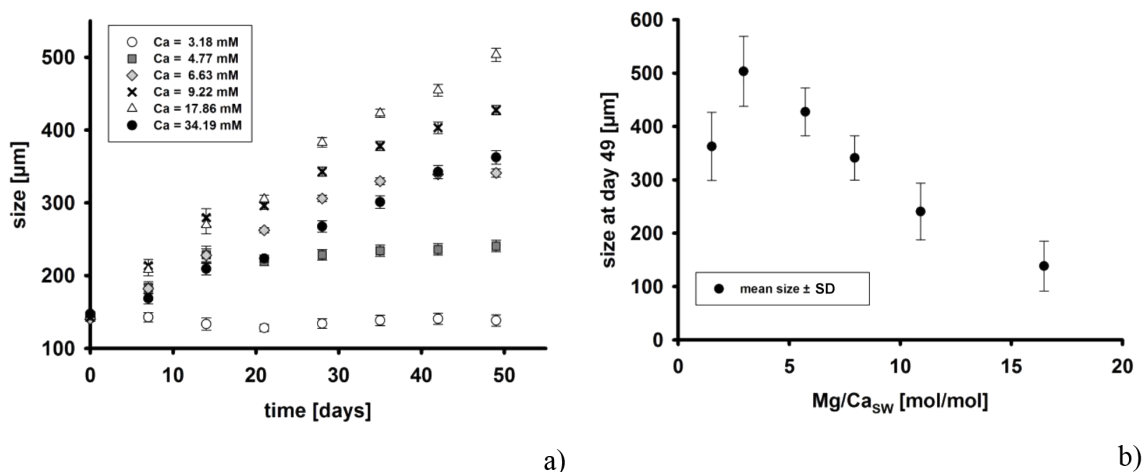
Figure 1. (a) Mean test size ±SE for all treatments vs. time in culture ($n = 37$–56). **(b)** Mean test size ±SD at the end of the experiment vs. seawater Mg / Ca.

2.8 Element measurements

Elemental concentrations were determined using laser-ablation inductively coupled plasma mass spectrometry (LA-ICP-MS). For this purpose, analyses were done on the Geo-Las 22Q Excimer laser (Lambda Physik), coupled to a sector field ICP-MS (Element 2, Thermo Scientific) at Utrecht University (Reichart et al., 2003). Prior to analyses, specimens were mounted on stubs with double-sided adhesive tape. Depending on the size of the chambers, the laser spot size was set to 80, 60 or 40 µm to ablate as much material as possible while at the same time avoiding contamination from adjacent chambers. From each replicate group in each of the treatments, four to six chambers of one to two specimens were analyzed, resulting in 50 to 65 measurements per treatment. Data from single-chamber measurements were calibrated against a glass standard (SRM NIST 610; Jochum et al., 2011). To assure high signal quality (e.g., to correct for drift), every 10–15 measurements two NIST standards were measured. The laser repetition rate was set to 7 Hz and the energy density was set to $\sim 1.2\,\mathrm{J\,cm^{-2}}$ when ablating calcite and to $\sim 5\,\mathrm{J\,cm^{-2}}$ when ablating glass. Elemental concentrations were calculated for ^{24}Mg, ^{26}Mg, ^{43}Ca and ^{44}Ca using the software GLITTER (version 4.4.3). A carbonate standard, produced in-house, with known Mg / Ca and Sr / Ca was measured at an energy density of $\sim 1.2\,\mathrm{J\,cm^{-2}}$ every 10–12 foraminiferal samples and allowed us to check for matrix effects that may result from switching between energy densities (Dueñas-Bohórquez et al., 2009, 2011). All profiles were evaluated individually and those parts of the profiles where ^{27}Al and/or ^{55}Mn (indicating potential contamination) were elevated were rejected. From a total of 305 ablations, 17 had to be discarded, either because of contamination or due to short ablation profiles, typically from the thinly calcified last chamber. Mg fractionation, expressed as

the partition coefficient for Mg (D_{Mg}), was calculated by dividing the Mg / Ca of the calcite (Mg / Ca$_{\mathrm{CC}}$) by the Mg / Ca of seawater (Mg / Ca$_{\mathrm{SW}}$):

$$D_{\mathrm{Mg}} = \frac{\mathrm{Mg / Ca_{CC}}}{\mathrm{Mg / Ca_{SW}}}. \tag{2}$$

3 Results

3.1 Morphological parameters

3.1.1 Size and growth rates

Figure 1a shows the growth of foraminifers in the different treatments. At very low [Ca] (3 mM), foraminifers did not grow (Fig. 1a). With increasing [Ca], growth rates progressively increased, whereas at highest seawater [Ca] (34 mM), growth rates were reduced again. At lower [Ca] (e.g., Ca = 5 and 7 mM), growth seemed to cease before the termination of the experiment, while in the treatments with higher [Ca] (e.g., Ca = 9 and 18 mM) growth continued throughout the experiment.

Figure 1b shows the final mean test size for the different treatments. The largest test size of 503 µm suggests that optimal growth conditions were attained at [Ca] = 17.9 mM and Mg / Ca$_{\mathrm{SW}}$ = 2.9, directly followed by the near-ambient control treatment at [Ca] = 9 mM and Mg / Ca = 5.7, with a final test size of 428 µm (Fig. 1b).

3.1.2 Size-normalized weight

Figure 2 shows size-normalized weight, a measure for test wall thickness, for the different treatments. Similar to growth, size-normalized weights were also highest (0.21 µg µm^{-1}) at seawater [Ca] = 9 mM and Mg / Ca$_{\mathrm{SW}}$ =
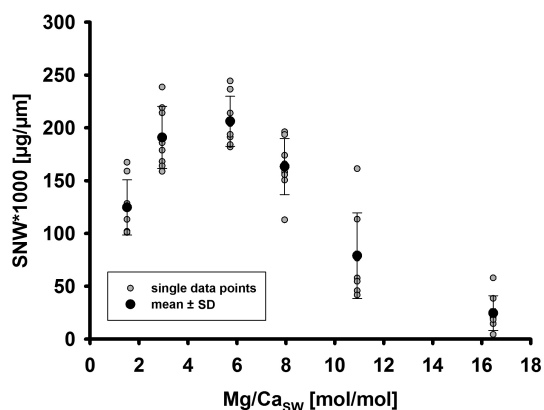
Figure 2. Size-normalized weight vs. seawater Mg / Ca ($n = 8$).

5.7. Seawater [Ca] lower or higher than this condition resulted in reduced size-normalized weight and hence test wall thicknesses.

3.2 Calcite Mg / Ca

Figure 3a shows the relationship between Mg / Ca$_{CC}$ and Mg / Ca$_{SW}$. With increasing Mg / Ca$_{SW}$ and thus decreasing seawater [Ca] (and decreasing Ω), Mg / Ca$_{CC}$ increases. This relationship can be described by a linear regression with a positive y intercept. The relationship between the distribution coefficient, D_{Mg}, and Mg / Ca$_{SW}$ is best described by an exponential decrease, approaching an asymptote (Fig. 3b).

4 Discussion

4.1 Growth rates and size-normalized weight

Growth rates ($\mu m \, d^{-1}$) varied substantially with seawater [Ca] (Fig. 1). Except for the treatment with highest seawater [Ca], increased [Ca] levels correlated with increased growth rates. Considering only the current data set by itself, one could conclude that increasing [Ca] causes faster growth until a certain toxic level at [Ca] > 18 mM. However, comparing the present data set with the one from Mewes et al. (2014), where the absolute [Mg] was varied and [Ca] was kept constant, shows that the calcium concentration by itself cannot be the primary driver of growth rates but that they are controlled by the Mg / Ca of seawater. To compare data in the present study with those from Mewes et al. (2014), growth rates (in $\mu m \, day^{-1}$) were derived from a linear regression curve fitted to the size data of the first 30 days (Fig. 4). It is not possible to derive growth rates from a linear regression line fitted to the time span of the whole experiment (49 days), due to the saturation of growth in the present study after 30 days (Fig. 1a). As a result, the time spans of growth between the two culture studies are different and do, furthermore, not allow a simple comparison of final test size.

Mewes et al. (2014) varied seawater [Mg] and kept [Ca] constant at 10 mM, observing a similar optimum at ambient Mg / Ca$_{SW}$. An increase of seawater [Mg] from ~ 50 to ~ 90 mM decreased growth rates even more than lowering [Mg] from ~ 50 to ~ 14 mM. The varying growth rates in the Mewes et al. (2014) data set at constant [Ca] clearly show that it is not the calcium concentration itself that is the primary driver of growth rates. Considering both data sets rather suggests that the seawater Mg / Ca$_{SW}$ ratio is the primary driver of growth rates and not the absolute concentrations of Ca or Mg. Apparently, the optimum Mg / Ca$_{SW}$ for foraminiferal growth is between 3 and 5 mol mol^{-1} (Fig. 4). In a similar study, Segev and Erez (2006) measured growth rates in *Amphistegina* spp. as a function of seawater Mg / Ca in terms of CaCO$_3$ addition, similarly concluding that the Mg / Ca ratio of seawater is the main driver of the specimens' growth rates. Their data suggest that the highest growth rate is reached at a Mg / Ca$_{SW}$ of ~ 1, while a ratio of ~ 0.5 was suboptimal. Because Mg is known to inhibit inorganic calcite precipitation, they concluded that *Amphistegina* spp. is able to precipitate its test more easily from seawater with lower Mg / Ca ratios. While this argument is based on a comparison with the inorganic system, their explanation for the decline in growth rate at a Mg / Ca$_{SW}$ of ~ 0.5 mol mol^{-1} is based on physiology, i.e., that a minimum of Mg is required for foraminiferal growth. This physiological explanation can in itself not fully explain our results because the lowest Mg / Ca$_{SW}$ in our studies (the present one and Mewes et al., 2014) was achieved through both elevating seawater [Ca] and lowering [Mg]. Interestingly, growth rates at the lowest Mg / Ca$_{SW}$ are lower in the case of the Ca-variable experiment, indicating that at this particular Mg / Ca the high Ca concentration may be more detrimental to growth than the low Mg concentration (Fig. 4). The latter observation can neither be explained in terms of inorganic calcite precipitation nor in terms of a minimum Mg requirement. However, it may be that high seawater [Ca] may be toxic for the cell (e.g., Martinez-Colon et al., 2009). Together, the results of Segev and Erez (2006) and those presented here strongly suggest that growth in *Amphistegina* spp. is influenced by the Mg / Ca$_{SW}$ ratio. With these data sets, it is currently impossible to determine the optimal Mg / Ca$_{SW}$ ratio for foraminiferal growth because the available data sets suggest a plateau rather than a clearly defined peak value. Our data set (Fig. 4) suggests an optimum between 3 and 5 mol mol^{-1} but may range from 2 to 5 mol mol^{-1}. The data set of Segev and Erez (2006) locates the optimum between 1 and 2.5 mol mol^{-1}. However, this is a potentially biased range because there are no data between a Mg / Ca$_{SW}$ of 2.5 and 5 mol mol^{-1}. This implies that these two data sets combined (Fig. 4, Segev and Erez, 2006) suggest an optimum between 1 and 5 mol mol^{-1}. While this might appear to be a large range, it is a reasonable interval from a physiological perspective because physiological optima usually comprise a range of values. Well-known examples are temperature,

a)

b)
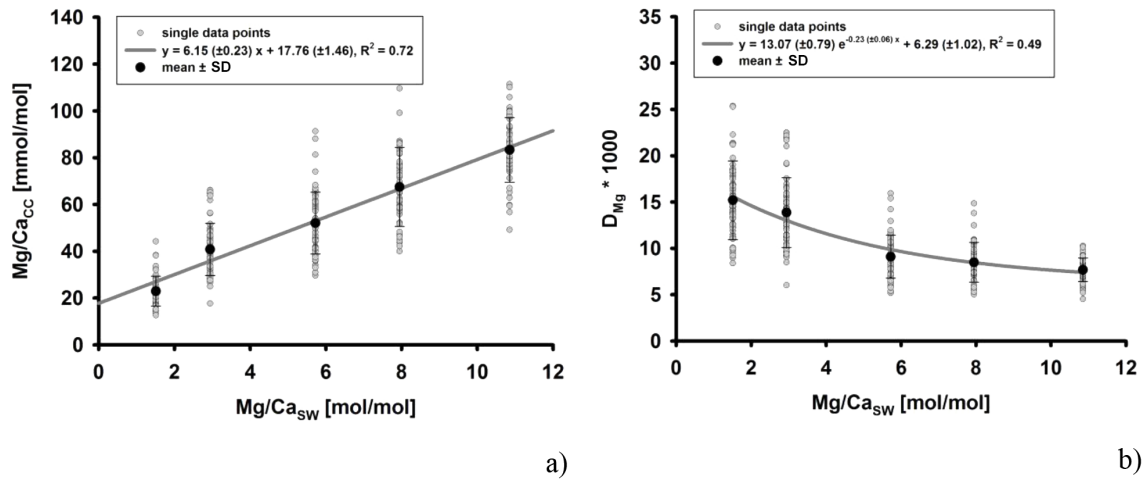
Figure 3. (a) Mg / Ca$_{CC}$ vs. Mg / Ca$_{SW}$ ([Ca] and thus Ω decreases with increasing Mg / Ca$_{SW}$) and **(b)** $D_{Mg} \times 1000$ vs. Mg / Ca$_{SW}$ ($n = 50$–65 ablations per treatment).
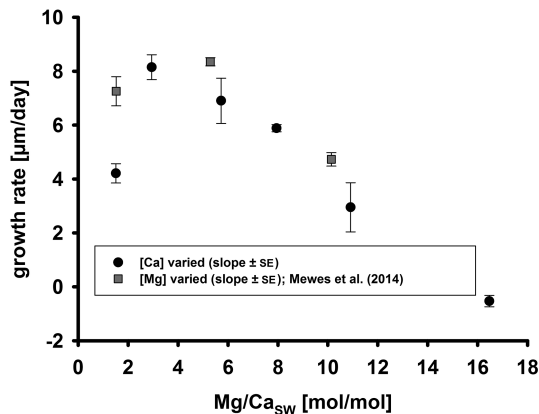
Figure 4. Growth rates (μm day^{-1}), derived from linear regression curves fitted to size data of the first 30 days in culture, vs. Mg / Ca$_{SW}$.
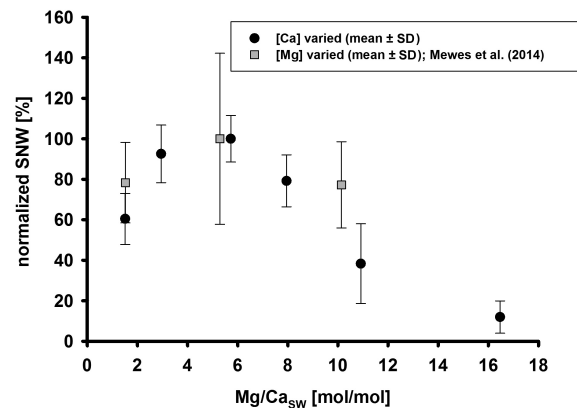

Figure 5. Normalized size-normalized weight (%) vs. Mg / Ca$_{SW}$.

light intensity and nutrient concentrations. The same argumentation also applies to SNW (Fig. 5). This is the first study showing the effect of Mg / Ca$_{SW}$ on foraminiferal SNW. The effect of Mg / Ca$_{SW}$ on foraminiferal SNW shows the same trend (optimum curve) as the effect of Mg / Ca$_{SW}$ on growth rates. Similar trends for growth rate and SNW in response to seawater carbonate-chemistry changes were described for another benthic foraminifer, namely *Ammonia tepida* (i.e., *A. aomoriensis*) (Keul et al., 2013). It should be emphasized that a comparison of absolute values for SNW or the growth rate between different experiments is challenging since observed values are highly variable, even under similar culture conditions. This problem is not confined to foraminifers but is also known from culture studies using coccolithophores (Hoppe et al., 2011). It is therefore reasonable to follow the recommendation of Hoppe et al. (2011) and base interpretations on response patterns, i.e., trends, rather than absolute values.

4.2 Calcite Mg / Ca

Our results show that Mg / Ca$_{CC}$ increases linearly with decreasing seawater [Ca] and, thus, with increasing Mg / Ca$_{SW}$ (Fig. 3a). A comparison with our previous study, where [Mg] was varied and [Ca] was kept constant (Mewes et al., 2014), shows a strong agreement between the two data sets (Fig. 6a). This suggests that test Mg / Ca$_{CC}$ is controlled by the ratio of Mg to Ca in seawater rather than by absolute concentrations. This result would be in accordance with a calcification mechanism based on seawater vacuolization if the Mg transport mechanism features Ca fractionation independent of seawater Mg or Ca concentrations. While this is a perfectly reasonable scenario, it makes little sense when considering the assumed function of this transport, i.e., Mg homoeostasis. In other words, if the behavior of the Mg transporter is compatible with our data, it cannot perform its alleged role. Calcification based on vacuolization might exclude Mg homoeostasis as a function of this transporter, and, instead, the func-

a)

b)
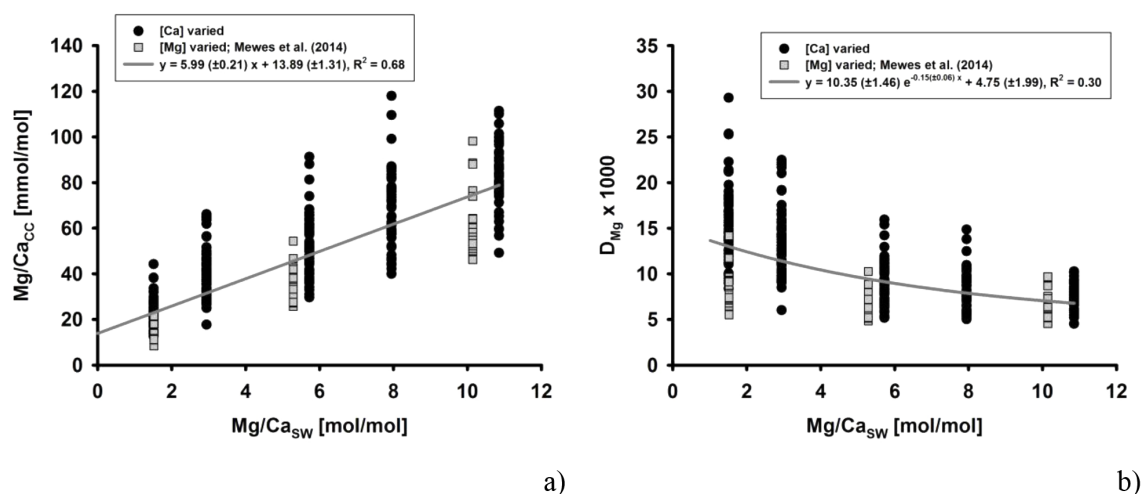
Figure 6. (a) Mg / Ca$_{CC}$ vs. Mg / Ca$_{SW}$. **(b)** D$_{Mg}$ × 1000 vs. Mg / Ca$_{SW}$. Grey lines represent functions fitted to the combined data set.

tion might merely be a lowering of the Mg / Ca ratio. Hence, the question of whether our data are compatible with a calcification mechanism based on the vacuolization of seawater, depends on the precise interpretation of this mechanism.

Foraminiferal Mg / Ca$_{CC}$ at varying Mg / Ca$_{SW}$ can be used to test the biomineralization model developed by Nehrke et al. (2013). This model assumes that foraminifers obtain the majority of Ca^{2+}, needed for calcification, via highly selective TMT and that the majority of the Mg^{2+} stems from (unfractionated) seawater leakage or vacuolar transport (i.e., PT). In contrast to the vacuole-based biomineralization model (e.g., Bentov and Erez, 2006; Bentov et al., 2009), the TMT–PT mixing model assumes that the percentage of ions transported via PT is very small compared to those delivered by TMT. Given that elements are not fractionated during the transport of vacuoles to the site of calcification, the contribution from vacuole-bound ions or seawater leakage plays a key role in determining the Mg / Ca$_{CC}$. The model explains the difference between low-, medium- and high-Mg calcite species via an increasing relative contribution of PT. As already suggested by Nehrke et al. (2013), the model predictions can be tested with culture studies such as this one.

The mixing model (Nehrke et al., 2013) predicts a linear relationship between Mg / Ca$_{CC}$ and Mg / Ca$_{SW}$, intersecting with the origin. As discussed by Mewes et al. (2014), the relationship between Mg / Ca$_{CC}$ and Mg / Ca$_{SW}$ is best described by a linear relationship with a positive intercept (Fig. 6a). At high Mg / Ca$_{SW}$ this relationship is in line with the mixing model (Nehrke et al., 2013). At very low Mg / Ca$_{SW}$, however, the present and our previous data have a positive y intercept, i.e., an increased D$_{Mg}$ (Fig. 6b), which is not predicted by the model of Nehrke et al. (2013) (for discussion, see Mewes et al., 2014). Here we present a refined flux-based model, which solves this problem (for the math-

ematical derivation see the Appendix). The model is based on the same assumptions as Nehrke et al. (2013): the total ion flux is divided into PT and TMT (mixing model). The fraction of the total flux of the divalent cations transported via PT is expressed as x (see Eq. A2). Similar to Nehrke et al. (2013), we assume no fractionation during passive transport, while we assume strong fractionation (frac) during TMT (see Eqs. A4 and A5). The Mg / Ca$_{CC}$ ratio of the precipitated calcite represents the Mg / Ca ratio of the two different fluxes (see Eq. A10). A further fundamental assumption is that Mg^{2+} replaces Ca^{2+} in the calcite lattice, i.e., in a given volume of calcite, the sum of Mg and Ca ions is constant. Based on data showing high-Mg areas in conjunction with organic layers in the shell, it was traditionally assumed that Mg^{2+} may be incorporated in the organic layers, rather than in the calcite lattice alone (Erez, 2003). However, by means of nano-scale synchrotron X-ray spectroscopy, Branson et al. (2013) showed that most of the Mg present in foraminiferal shells replaces Ca in the calcite lattice. Therefore, the assumption that the sum of Mg and Ca is constant is justified.

Based on the above assumptions the refined flux-based model yields calcite Mg / Ca

$$\left(\frac{Mg^{2+}}{Ca^{2+}}\right)_{SW} = R_{SW}\left[\frac{\text{frac}\,(1-x)+x+\text{frac}\cdot R_{SW}}{1+(1-x+\text{frac}\cdot x)\,R_{SW}}\right]. \quad (3)$$

The curve (Fig. 7a) can be fitted over the whole R_{SW} (= Mg / Ca$_{SW}$) with TMT fractionation frac = 0.005 and a contribution of PT to the total ion flux x = 0.02. TMT fractionation, i.e., 0.005 (= frac), is weaker than the one assumed in the previous model (0.0001; Nehrke et al., 2013). This is a reasonable modification because Mg TMT fractionation is not known in either coccolithophores or Foraminifera and typical Ca channels display a range of Mg fractionation (e.g., White, 2000).
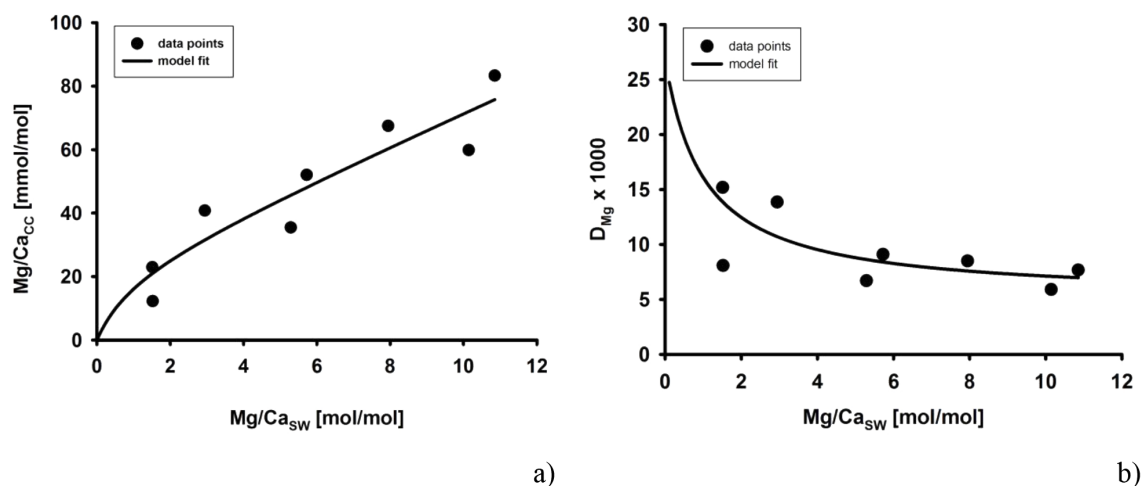
Figure 7. Model fit to the data of our present and previous studies (Mewes et al., 2014) for **(a)** Mg / Ca$_{CC}$ vs. Mg / Ca$_{SW}$ and **(b)** D$_{Mg}$ × 1000 vs. Mg / Ca$_{SW}$.

The partition coefficient for Mg is given by

$$D_{Mg^{2+}} = \left(\frac{Mg^{2+}}{Ca^{2+}}\right)_{CC} \Big/ R_{SW} \qquad (4)$$
$$= \frac{frac(1-x) + x + frac \cdot R_{SW}}{1 + (1 - x + frac \cdot x) R_{SW}}.$$

This refined flux-based model predicts both the trend of Mg / Ca$_{CC}$ vs. Mg / Ca$_{SW}$ and D_{Mg} vs. Mg / Ca$_{SW}$. The dependence of D_{Mg} on Mg / Ca$_{SW}$, especially, is interesting because the trend observed here (Figs. 6b and 7b) was also reported for inorganically precipitated calcite (Mucci and Morse, 1983). Segev and Erez (2006) already noted this curious fact. They commented: "A physiological mechanism sensitive to ratio ... remains to be explored" (Segev and Erez, 2006). We present such a physiological mechanism, which comprises transmembrane transport and seawater vacuolization. Our refined flux-based model for major- and minor-element incorporation therefore represents a promising new way of interpreting foraminiferal-element-to-calcium ratios. Future research should hence be concerned with the question of whether the behavior of other elements can be reconciled with our model.

5 Summary

Our study showed optimum growth performance of *Amphistegina lessonii* at near-ambient Mg / Ca$_{SW}$. Growth rates, test wall thickness and also test Mg / Ca$_{CC}$ are not controlled by absolute seawater [Ca] and [Mg] but by their ratio in seawater. We provide further support for the biomineralization model recently developed by Nehrke et al. (2013) and present a refined flux-based model which predicts our experimentally determined dependence of Mg / Ca$_{CC}$ on Mg / Ca$_{SW}$.

Appendix A: Refined TMT–PT mixing model

The transport of Mg^{2+} and Ca^{2+} in our flux-based model is described in terms of the total flux of the bivalent cations:

$$F_{CAT} = F_{Ca^{2+}} + F_{Mg^{2+}}. \tag{A1}$$

The total ion flux is subdivided into passive transport (PT) and transmembrane transport (TMT). Assuming that a fraction x of the total flux is transported via PT, the fluxes of bivalent cations for both transport pathways are expressed as

$$F_{PT} = F_{PT,Ca^{2+}} + F_{PT,Mg^{2+}} = x F_{CAT}, \tag{A2}$$

$$F_{TMT} = F_{TMT,Ca^{2+}} + F_{TMT,Mg^{2+}} = (1-x) F_{CAT}. \tag{A3}$$

The contribution of Ca^{2+} and Mg^{2+} to PT and TMT is controlled by fractionation during transport. It is assumed that no fractionation takes place during passive transport, but strong fractionation (frac) takes place during TMT. Based on this assumption the ratios of Ca^{2+} and Mg^{2+} fluxes are given by

$$\frac{F_{PT,Mg^{2+}}}{F_{PT,Ca^{2+}}} = R_{SW}, \quad \frac{F_{TMT,Mg^{2+}}}{F_{TMT,Ca^{2+}}} = \text{frac} \cdot R_{SW}, \tag{A4}$$

where R_{SW} is the seawater Mg / Ca. Combining Eqs. (A2)–(A5) yields the Ca^{2+} and Mg^{2+} fluxes for the PT and TMT pathways:

$$F_{PT,Mg^{2+}} = \frac{R_{SW}}{1 + R_{SW}} x \cdot F_{CAT}, \tag{A5}$$

$$F_{PT,Ca^{2+}} = \frac{1}{1 + R_{SW}} x \cdot F_{CAT}, \tag{A6}$$

$$F_{TMT,Mg^{2+}} = \frac{\text{frac} \cdot R_{SW}}{1 + \text{frac} \cdot R_{SW}} (1-x) F_{CAT}, \tag{A7}$$

$$F_{TMT,Ca^{2+}} = \frac{1}{1 + \text{frac} \cdot R_{SW}} (1-x) F_{CAT}. \tag{A8}$$

The Mg / Ca$_{CC}$ ratio of the precipitated calcite represents the Mg / Ca ratio of the ion fluxes:

$$\left(\frac{Mg^{2+}}{Ca^{2+}}\right)_{CC} = \frac{F_{TMT,Mg^{2+}} + F_{PT,Mg^{2+}}}{F_{TMT,Ca^{2+}} + F_{PT,Ca^{2+}}} \tag{A9}$$

$$= \frac{\frac{\text{frac} \cdot R_{SW}}{1 + \text{frac} \cdot R_{SW}} (1-x) F_{CAT} + \frac{R_{SW}}{1 + R_{SW}} x \cdot F_{CAT}}{\frac{1}{1 + \text{frac} \cdot R_{SW}} (1-x) F_{CAT} + \frac{1}{1 + R_{SW}} x \cdot F_{CAT}},$$

which can be written as

$$\left(\frac{Mg^{2+}}{Ca^{2+}}\right)_{CC} = R_{SW} \left[\frac{\text{frac}\,(1-x) + x + \text{frac} \cdot R_{SW}}{1 + (1 - x + \text{frac} \cdot x)\,R_{SW}}\right]. \tag{A10}$$

Equation (A11) indicates that the calcite Mg / Ca depends on the seawater Mg / Ca but not on the total flux of the bivalent cations (F_{CAT}). This explains why test Mg / Ca is controlled by the ratio of Mg and Ca but not by their absolute concentrations in seawater. The partition coefficient for Mg ($D_{Mg^{2+}}$) is defined with respect to seawater Mg / Ca; thus,

$$D_{Mg^{2+}} = \left(\frac{Mg^{2+}}{Ca^{2+}}\right)_{CC} \bigg/ R_{SW} \tag{A11}$$

$$= \frac{\text{frac}(1-x) + x + \text{frac} \cdot R_{SW}}{1 + (1 - x + \text{frac} \cdot x)\,R_{SW}}.$$

Edited by: H. Kitazato

References

Bentov, S. and Erez, J.: Impact of biomineralization processes on the Mg content of foraminiferal shells: A biological perspective, Geochem. Geophys. Geosy., 7, 1–11, 2006.

Bentov, S., Brownlee, C. and Erez, J.: The role of seawater endocytosis in the biomineralization process in calcareous foraminifera, P. Natl. Acad. Sci., 106, 21500–21504, 2009.

Branson, O., Redfern, S. A., Tyliszczak, T., Sadekov, A., Langer, G., Kimoto, K., and Elderfield, H.: The coordination of Mg in foraminiferal calcite, Earth Planet. Sci. Lett., 383, 134–141, 2013.

Broecker, W. and Yu, J.: What do we know about the evolution of Mg to Ca ratios in seawater?, Paleoceanography 26, PA3203, doi:10.1029/2011PA002120, 2006.

de Nooijer, L. J., Langer, G., Nehrke, G., and Bijma, J.: Physiological controls on seawater uptake and calcification in the benthic foraminifer *Ammonia tepida*, Biogeosciences, 6, 2669–2675, doi:10.5194/bg-6-2669-2009, 2009.

de Nooijer, L. J., Spero, H. J., Erez, J., Bijma, J., and Reichart, G. J.: Biomineralization in perforate Foraminifera, Earth-Sci. Rev., 135, 48–58, 2014.

Dueñas-Bohórquez, A., da Rocha, R. E., Kuroyanagi, A., Bijma, J., and Reichart, G. J.: Effect of salinity and seawater calcite saturation state on Mg and Sr incorporation in cultured planktonic foraminifera, Mar. Micropaleontol., 73, 178–189, 2009.

Dueñas-Bohórquez, A., Da Rocha, R. E., Kuroyanagi, A., De Nooijer, L. J., Bijma, J., and Reichart, G. J.: Interindividual variability and ontogenetic effects on Mg and Sr incorporation in the planktonic foraminifer *Globigerinoides sacculifer*, Geochim. Cosmochim. Acta, 75, 520–532, 2011.

Erez, J: The Source of Ions for Biomineralization in Foraminifera and Their Implications for Paleoceanographic Proxies, Reviews in Mineralogy and Geochemistry, 54, 115–149, 2003.

Ernst, S., Janse, M., Renema, W., Kouwenhoven, T., Goudeau, M. L., and Reichart, G. J.: Benthic foraminifera in a large Indo-Pacific coral reef aquarium, J. Foramin. Res., 41, 101–113, 2011.

Evans, D. and Müller, W.: Deep time foraminifera Mg / Ca paleothermometry: Nonlinear correction for secular change in seawater Mg / Ca, Paleoceanography, 27, PA4205, doi:10.1029/2012PA002315, 2012.

Hardie, L. A.: Secular variation in seawater chemistry: An explanation for the coupled secular variation in the mineralogies of marine limestones and potash evaporites over the past 600 my, Geology, 24, 279–283, 1996.

Hoppe, C. J. M., Langer, G., and Rost, B.: *Emiliania huxleyi* shows identical responses to elevated pCO$_2$ in TA and DIC manipulations, J. Exp. Mar. Biol. Ecol., 406, 54–62, 2011.

Jochum, K. P., Weis, U., Stoll, B., Kuzmin, D., Yang, Q. C., Raczek, I., Jacob, D. E., Stracke, A., Birbaum, K., Frick, D. A., Gunther, D., and Enzweiler, J.: Determination of reference values for NIST SRM 610-617 glasses following ISO guidelines, Geostand. Geoanal. Res., 35, 397–429, 2011.

Kester, D. R., Duedall, I. W., Connors, D. N., and Pytkowicz, R. M.: Preparation of artificial seawater, Limnol. Oceanogr., 12, 176–179, 1967.

Keul, N., Langer, G., de Nooijer, L. J., and Bijma, J.: Effect of ocean acidification on the benthic foraminifera *Ammonia* sp. is caused by a decrease in carbonate ion concentration, Biogeosciences, 10, 6185–6198, doi:10.5194/bg-10-6185-2013, 2013.

Lear, C. H., Elderfield, H., and Wilson, P. A.: Cenozoic deep-sea temperatures and global ice volumes from Mg / Ca in benthic foraminiferal calcite, Science, 287, 269–272, 2000.

Martínez-Colón, M., Hallock, P., and Green-Ruíz, C.: Strategies for using shallow-water benthic foraminifers as bioindicators of potentially toxic elements: a review, J. Foramin. Res., 39, 278–299, 2009.

Mewes, A., Langer, G., de Nooijer, L. J., Bijma, J., and Reichart, J. G.: Effect of different seawater Mg^{2+} concentrations on calcification in two benthic foraminifers, Mar. Micropaleontol., 113, 56–64, 2014.

Mucci, A. and Morse, J. W.: The incorporation of Mg^{2+} and Sr^{2+} into calcite overgrowths: influences of growth rate and solution composition, Geochim. Cosmochim. Acta, 47, 217–233, 1983.

Nehrke, G., Keul, N., Langer, G., de Nooijer, L. J., Bijma, J., and Meibom, A.: A new model for biomineralization and trace-element signatures of Foraminifera tests, Biogeosciences, 10, 6759–6767, doi:10.5194/bg-10-6759-2013, 2013.

Nürnberg, D., Bijma, J., and Hemleben, C.: Assessing the reliability of magnesium in foraminiferal calcite as a proxy for water mass temperatures, Geochim. Cosmochim. Acta, 60, 803–814, 1996.

Raitzsch, M., Dueñas-Bohórquez, A., Reichart, G.-J., de Nooijer, L. J., and Bickert, T.: Incorporation of Mg and Sr in calcite of cultured benthic foraminifera: impact of calcium concentration and associated calcite saturation state, Biogeosciences, 7, 869–881, doi:10.5194/bg-7-869-2010, 2010.

Reichart, G. J., Jorissen, F., Anschutz, P., and Mason, P. R.: Single foraminiferal test chemistry records the marine environment, Geology, 31, 355–358, 2003.

Segev, E. and Erez, J.: Effect of Mg / Ca ratio in seawater on shell composition in shallow benthic foraminifera, Geochem. Geophys. Geosy., 7, 1–8, 2006.

Signes, M., Bijma, J., Hemleben, C., and Ott, R.: A model for planktic foraminiferal shell growth, Paleobiology, 19, 71–91, 1993.

Ter Kuile, B., Erez, J., and Padan, E.: Mechanisms for the uptake of inorganic carbon by two species of symbiont-bearing foraminifera, Mar. Biol., 103, 241–251, 1989.

White, P. J.: Calcium channels in higher plants, Biochimica et Biophysica Acta (BBA)-Biomembranes, 1465, 171–189, 2000.